Original Article

Quality Assessment of Computed Tomography Images using a Channelized Hoteling Observer: Optimization of Protocols in Clinical Practice

Mohammad Reza Choopani[1], Iraj Abedi[2], Fatemeh Dalvand[3]

[1]Department of Radiology, Isfahan University of Medical Sciences, Isfahan, Iran, [2]Department of Medical Physics, School of Medicine, Isfahan University of Medical Sciences, Isfahan, Iran, [3]Department of Radiation Engineering, Shahid Beheshti University, Tehran, Iran

Abstract

Background: This study investigated the feasibility of channelized hoteling observer (CHO) model in computed tomography (CT) protocol optimization regarding the image quality and patient exposure. While the utility of using model observers such as to optimize the clinical protocol is evident, the pitfalls associated with the use of this method in practice require investigation.

Materials and Methods: This study was performed using variable tube current and adaptive statistical iterative reconstruction (ASIR) level (ASIR 10% to ASIR 100%). Various criteria including noise, high-contrast spatial resolution, CHOs model were used to compare image quality at different captured levels. For the implementation of CHO, we first tuned the model in a restricted dataset and then it to the evaluation of a large dataset of images obtained with different reconstruction ASIR and filtered back projection (FBP) levels.

Results: The results were promising in terms of CHO use for the stated purposes. Comparisons of the noise of reconstructed images with 30% ASIR and higher levels of noise in rebuilding images using the FBP approach showed a significant difference ($P < 0.05$). The spatial resolution obtained using various ASIR levels and tube currents were 0.8 pairs of lines per millimeter, which did not differ significantly from the FBP method ($P > 0.05$).

Conclusions: Based on the results, using 80% ASIR can reduce the radiation dose on lungs, abdomen, and pelvis CT scans while maintaining image quality. Furthermore using ASIR 60% only for the reconstruction of lungs, abdomen, and pelvis images at standard radiation dose leads to optimal image quality.

Keywords: Channelized hoteling observer, computed tomography, radiation dose

Address for correspondence: Dr. Iraj Abedi, Department of Medical Physics, School of Medicine, Isfahan University of Medical Sciences, Isfahan, Iran.
E-mail: Iraj_abedi@yahoo.com
Submitted: 03-Nov-2021; **Revised:** 16-Jan-2022; **Accepted:** 31-Jan-2022; **Published:** 27-Jan-2023

Introduction

The increasing use of computed tomography (CT) scans raises concerns regarding the possible health impact of radiation exposure owing to CT scans. Previous studies have shown that while CT accounts for only 15% of all imaging tests, it accounts for more than 75% of all radiation.[1-3] On the other hand, dose reduction comes at the expense of increased noise. Thus, in recent years, the technological challenge has been to lower the dose while preserving the image diagnostic quality.[4,5] Advances in CT technology have focused on minimizing radiation exposure while maintaining diagnostic performance. Recent advances have resulted in significant reductions in radiation exposure in many clinical settings. Over the past decade, iterative reconstruction (IR) techniques have become increasingly popular as a mechanism

Access this article online

Quick Response Code:

Website: www.advbiores.net

DOI: 10.4103/abr.abr_353_21

How to cite this article: Choopani MR, Abedi I, Dalvand F. Quality assessment of computed tomography images using a channelized hoteling observer: Optimization of protocols in clinical practice. Adv Biomed Res 2023;12:8.

for reducing radiation exposure.[6] The adaptive statistical iterative reconstruction (ASIR) algorithm (GE Healthcare, Waukesha, WI, USA) is a hybrid IR that involves filtered back projection (FBP) images and only models the photon and electronic noise statistics, which mainly affect the image noise. In fact, the ASIR technique uses various complicated mathematical models to eliminate noise from low-dose images and maintain or improve image quality.

Although just using the ASIR technique in reconstruction can significantly reduce image noise, increasing the ASIR in image reconstruction can lead to artifacts and decreased the ability to detect objects with low contrast.[6,7] In fact, radiologists decide how much ASIR to use (as a percentage) in image reconstruction in each imaging test. In many protocols that use the ASIR reconstruction technique, the value is set between 10% and 40%.[8] It means that the exposure can be reduced by 10%–40% without jeopardizing image quality.

Image quality can be measured by a human trying to make a diagnosis or a model observer adapted to predict the performance of the human observer. However, human observer-based studies are resource-intensive and show significant intra-observer and inter-observer variability. With the ability to extract as much statistical information as possible from the images, computer model observers can be used as convenient and aim proxies. Of people to predict and/or define their expected performance.[2,9] Recent studies have widely applied this latter approach for image quality evaluation and in CT. Observer models, such as channelized hoteling observers (CHOs), are one method of image quality assessment that have been evaluated in studies in recent decades.[10,11] Previous studies showed that the results obtained from CHO models were highly correlated with the results reported by the human observer and well predicted the performance of the human observer.[12]

Most previous studies[6-8] have examined the optimization of the ASIR regeneration technique to reduce the radiation dose. However, this technique can also be used to improve image quality. However, increasing the level of ASIR reconstruction to improve image quality can lead to artifacts and reduced low contrast resolution. Therefore, this study aimed to optimize the ASIR technique to reduce the radiation dose and increase image quality in the lung, abdominal, and pelvis CT. Furthermore, this study investigated the feasibility of a CHO model in a CT protocol optimization program to ensure image quality and patient exposure for ASIR techniques in lung and abdominopelvic CT examinations.

Materials and Methods

Data acquisition

This study included 50 patients (29 men and 21 women) aged 27–51 years. Lung and abdominopelvic CT scans were obtained from all eligible patients. The BMMD-7 phantom consists of four sections used to evaluate the parameters of low contrast resolution, spatial resolution, noise, and accuracy of the CT number. All experiments in this study were performed using a 64-slice scanner (Light Speed VCT, GE Healthcare, 2016). The patients participating in this study were imaged according to the scan parameters shown in Table 1. The tube current ranged from 175 to 466 mA for the lung images and from 175 to 650 mA for the abdominopelvic images. In addition, the BMMD-7 phantom was scanned with a tube current of 200 mA according to the recommended scan parameters for images of the lungs, abdomen, and pelvis [Table 1]. To investigate the effect of ASIR on the radiation dose, the phantom was re-scanned at tube currents of 150, 100, and 40 mA without changing the other radiation conditions.

Image reconstruction

All raw scan data related to patient imaging were reconstructed using the FBP method and its combination with different levels of the ASIR technique (0% to 100%). In addition, each of the four raw scan datasets related to phantom imaging (200, 140, 100, and 40 mA) were reconstructed using FBP and ASIR (10% to 100%). A total of 340 phantom images and 1650 (50 patients × 33 images per patient) patient images were obtained according to the different imaging parameters and reconstructions.

Channelized hoteling observer model

The observer model used in this study was implemented in MATLAB (MATLAB R2015a). In the CHO model, the detection was considered to confirm of one of two unique hypotheses: H_0 (no signal) and H_1 (signal). The information of the observed image (g) is given in Equation 1.

$$Hh: G = hx + b, h = 0,1$$

where x and b indicate the known signal and background, respectively, and the binary variable "h" reflects the presence or absence of the signal. Then, a two-dimensional image (test image, signal, or background) was displayed using a vector by vertical concatenation. If the observed image has a pixel, its vector version (g) is M × 1.[13] The addition of a channel mechanism to predict human performance has been proposed by embedding channels in the frequency domain thought to exist in human visual systems.[14] The use of channels involves multiplying images using a series of channel-pattern images. If we assume an overall channel image "L" and that each channel image is like an M × 1 vector, a numerical value is obtained when applying each channel vector in the vector image. For example (Equation 1):

Table 1: The scan parameters

Scanning parameters	Value's
Tube voltage	100
Tube current	200
Rotation time	0.5
Slice thickness	5
Matrix	512×512
Pitch ratio	1
Automatic exposure	On

$V_i = u_i^t g$

In which "u_ii" is the trusted channel and "vi" is the answer "I" the trustworthy channel. Adding channel responses results in a channel data vector:

V= (v_1, v_2, v_3, vL)

The CHO statistical criterion is given by the following equation3:

$$\lambda = w_{CHO}^T v$$

Where (Equation 4):

$$w_{CHO}^T = S^{-1}(\bar{v}_1 - \bar{v}_0)$$

And $\bar{v}_1 = U^T \bar{g}_1, and\ \bar{v}_0 = U^T \bar{g}_0$ are the total average of the channeled vectors are the images of the existing signal and the missing signal, respectively.

Also (Equation 5),

$$S = \frac{1}{2}[K_1 + K_0]$$

where K_1 and K_0, are the covariance for the channel images of the existing signal and the missing signal, respectively.

In addition, the figure of merit (FOM) was calculated to describe the CHO detection function. The area under the curve (AUC) is a type of FOM that is calculated as the sum of the area under the receiver operating characteristic (ROC) curve. In cases where the AUC is not close to one, the AUC was estimated and then converted to detectability (signal-to-noise AUC, SNRAUC) according to the following equation 6:[15]

$$SNR_{AUC} = erf^{(-1)}(2\text{AUC} - 1)$$

Two-alternative forced choice study

From the images obtained from the phantom, regions of interest (ROIs) measuring 128 × 128 pixels and a field of view of 6.2 cm × 2.2 cm were drawn. Some of these ROIs were around the contrast bars, while others were on signal-less images. After extracting the ROIs, the obtained images were provided to the human observers and the observer model for the two-alternative forced choice (2AFC) studies. A total of 17 2AFC studies were performed, including four studies on FBP (4 mA configuration) and 13 studies on ASIR (4 mA configuration and 10 ASIR reconstruction levels). Each 2AFC study consisted of 80 trials in which one signal-less image and one signal image were placed side by side and the human observers and observer model determined which image had the signal.

Evaluation performance of the channelized hoteling observer in two-alternative forced choice studies

To evaluate the performance of the CHO model in the 2AFC experiment, we obtained the AUC values with and without the signal by calculating the signal-to-noise ratio or the area under the ROC curve. This value represented the percentage of correct decisions made by the CHO model in the 2AFC experiment.

Human observer tests

In this study, the 2AFC method was used to estimate the human observer performance. In each test, we randomly selected a signal-present image and a signal-absent image from the ROIs extracted in the CHO experiment. First, five samples of high-quality signal images were shown to three experienced, board-licensed radiologists (observers), who were asked to identify the characteristics of the signal area (size, shape, contrast, and location). Then, on a workstation with constant conditions in terms of ambient light and screen contrast, images of the same conditions were randomly provided to the observers. All observers were required to observe the images at a distance of 50–60 cm from the monitor. All abdominal CT scan images with window level of 40 and 400 window width of and lung CT scan images with window level of 700 and window width of 1700 were displayed for the observers to select the image containing the signal. In addition, the observers were asked to rate their confidence in the results of the qualitative analysis for each image using a six-part scale (0–5.5, with 5.5 indicating the highest confidence). Thus, 80 2AFC experiments were performed for each series of images under the same conditions. The percentage correct (PC) was defined as the number of correct decisions among the total number of decisions (80). The PC obtained from the 2AFC test was equivalent to the AUC.

Qualitative analysis

All image data obtained from the patients were analyzed by three experienced radiologists in a workstation under constant conditions in terms of ambient light. The images were provided to the observers at random. The observers were blinded to the scan parameters and retrieval method. The observers were only allowed to change the image magnification. To compare their quality, the images were displayed on a monitor in a 1 × 2 matrix. The reconstructed image was kept fixed by the FBP method as a comparison reference and the reconstructed images were replaced with different ASIR levels. The abdominopelvic images were displayed with a window level of 40 and a window width of 400, while the lung images were displayed with a window level of 700 and a window width of 1700. All parameters used in the subjective quality assessment are shown in Table 2. Similar to the study by Singh,[16] aortic wall resolution was used to evaluate the sharpness of the images. In addition to the presence of artifacts, Sagara *et al*.[17] also used a three-part scale.

Noise and noise power spectrum

The noise was marked on images of the uniform BMMD-7 CT module as the standard deviation (SD) of the pixel values in a square ROI located in the center of the phantom module. To calculate the level of noise, the size of the ROI was 25 × 25 pixels at the center of the image as described by shah SM.[18] Peach of the SD values in the present study was calculated based on 16 image replicates.

Lee and Kim[19] defined noise power spectrum (NPS) as the variance distribution of images across various spatial frequency components that are present in image noise. To carry out an NPS analysis, four 128 × 128-pixel ROIs were derived from each

Table 2: Grading scale for subjective image quality evaluation

Qualitative grading scale	Image quality				
	Sharpness	Subjective image noise	Artifact	Diagnostic acceptability	Visibility of small structure*
1	Blurry	Unacceptable noise	Present and affecting image interpretation	Unacceptable	Very poor
2	Poorer than average	Above average noise	Present but not affecting interpretation	Suboptimal	Suboptimal
3	Average	Average noise	Absent	Average	Acceptable
4	Better than average	Less than average noise		Above average	Above average
5	Sharpest	Minimum or no noise		Superior	Excellent

reconstructed image. Each ROI overlaps its close N/2-pixel neighbors in the vertical and horizontal directions. Sixteen replicated images were used to obtain a dependable resultant NPS curve, which led to a collection of 64 ROIs (16 × 4 × 128 × 128 arrays) employed to calculate each of the NPSs.

Then, the calculation technique suggested by Metheny[20] was performed (Equation 1).

$$NPS(fx, fy) = \frac{[FFT_{2D}(f_x, f_y)]2}{N^2_{FFT}} \Delta p^2$$

Where Δp represents the size of each pixel in the reconstructed image and FTN is the number of points employed in fast fourier transform (FFT) operations.

First, the array total variance (i.e., the square of the SD) was computed. Next, to exclude the mean value offset before using Eq.(1) on each ROI, the mean of each ROI was calculated and then subtracted from each of the pixels of that ROI. To execute the two-dimensional FFT operation, $NFFT^2 = 128^2$ points were employed. Subsequently, to obtain a normalized two-dimensional NPS curve, the two-dimensional NPS for each of the ROIs was normalized and averaged using the total variance.

The radial symmetry of the normalized two-dimensional NPS curve allows it to be transformed into a one-dimensional NPS curve. This was done by averaging the values of the two-dimensional NPS (*fx*, *fy*) in proportion to an identical radial frequency *fr*, which is expressed by Equation 2.

$$F_r = \sqrt{f_x^2} + f_y^2$$

Hence, the result is a one-dimensional NPS (*fr*) curve that is smoothed using a two-dimensional to one-dimensional operation.

High-contrast spatial resolution

High-contrast spatial resolution (i.e., limiting spatial resolution) is defined as the minimum resolvable diameter of an object within a uniform medium whose density differs from its background, as determined using an in-house fabricated high-contrast resolution phantom. A linear array was considered for each row of image objects. Two neighboring objects can be seen independently when the signal value varies with the distance between the two objects. Thus, a gradient along the X-axis is required to identify most variations. The differential values and SDs of each array are then calculated and placed in that array. The row can be noted when the number achieved for each row is higher than the threshold value. This operation was repeated in consequent rows to obtain the number of rows distinguishable from each image.

Results

Radiation dose

The CT dose index volume ($CTDI_{vol}$) in low-dose CT imaging with ASIR reconstruction at 150, 100, and 40 mA tube currents were 14.4, 9.6, and 4.8 mGy, respectively. In addition, the $CTDI_{vol}$ value in standard-dose imaging (200 mA tube current) was 12.56 mGy.

Quantitative evaluation

Noise

As shown in Figure 1, an increase in the level of ASIR reconstruction from 10% to 100% resulted in continuously reduced image noise ($P < 0.05$). In addition, the mean noise in the images obtained from the phantom with tube currents of 140, 100, and 40 mA reconstructed at ASIR levels of 30%, 50%, and 80% were 4.73 ± 0.31in abdominopelvic imaging and 17.33 ± 0.34 in lung imaging, which did not differ significantly from the noise in the images obtained at the standard radiation dose and reconstructed by the FBP method ($P > 0.05$).

Noise power spectrum

FFT techniques were employed to infer the NPS from the obtained images. The obtained results suggest that Image-J processing version 1.51 can be utilized to calculate the NPS with confidence. Figure 2 shows the NSP curves for different levels of ASIR reconstruction, which were normalized to the NPS curves for the FBP reconstruction. The NPS results showed that by increasing the level of ASIR reconstruction, the NPS ratio value decreased in the spatial frequency range of 0.4–0.8.

Spatial resolution

The results of human and model observers showed that the spatial resolution of the images did not change significantly with increasing ASIR reconstruction levels under constant

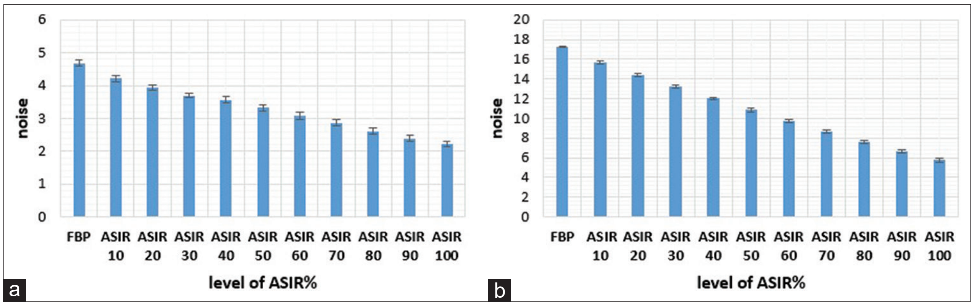

Figure 1: The effect of adaptive statistical iterative reconstruction reconstruction technique on noise. (a) Mean noise in abdominopelvic images. (b) Mean noise in lung images

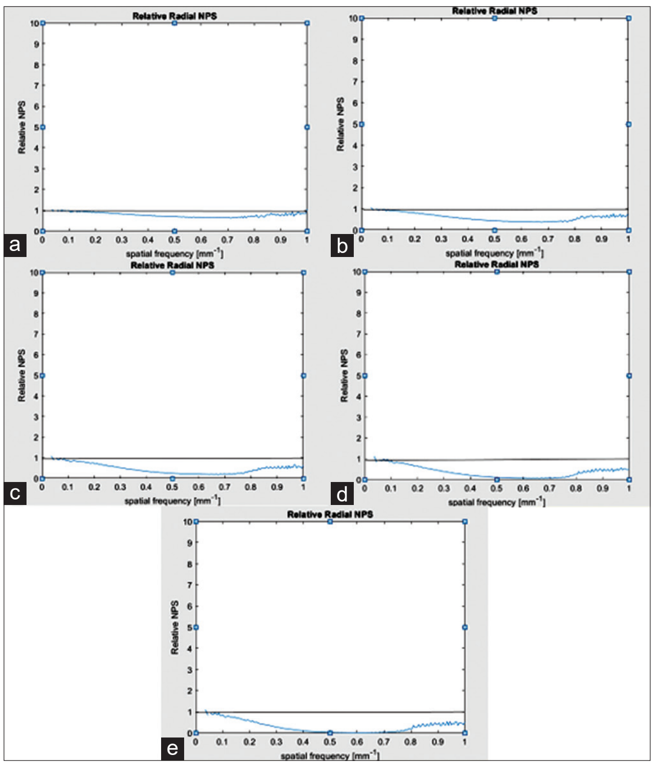

Figure 2: Noise power spectrum results for different levels of adaptive statistical iterative reconstruction reconstruction normalized to filtered back projection reconstruction. (a) 20% adaptive statistical iterative reconstruction, (b) 40% adaptive statistical iterative reconstruction, (c) 60% adaptive statistical iterative reconstruction, (d) 80% adaptive statistical iterative reconstruction, (e) 100% adaptive statistical iterative reconstruction

radiation conditions (P < 0.05). In addition, the spatial resolution of images obtained with low radiation doses and reconstructed with ASIR levels of 30%, 50%, and 80% (0.8 pairs of lines per millimeter) was approximately equivalent to the spatial resolution of images obtained at standard radiation doses and reconstructed by the FBP method (one pair of lines per millimeter). The intraclass correlation coefficient, which indicates the degree of agreement between the results reported by the observers, was 0.801. In addition, there was a statistically significant (P = 0.004) and moderate relationship (Pearson correlation coefficient = −0.468) between the values reported by the human and model observers.

Validation of the channelized hoteling observer model observer

Figure 3 shows a comparison of PC values in the 2AFC test for the human observer and the model observed in the lung and abdomen-pelvic examinations. The results indicated that human and model observations had a high correlation for four levels of tube current in both imaging examinations. The Pearson correlation coefficients for FBP reconstruction in lung and abdominopelvic examinations were 0.998 and 0.984, respectively. In addition, the PC values obtained from human and model observations at different levels of ASIR reconstruction were laos highly correlated. The Pearson correlation coefficients for ASIR reconstruction in lung and abdominopelvic examinations were 0.927 and 0.998, respectively.

Impact of adaptive statistical iterative reconstruction reconstruction on two-alternative forced choice task

Figure 4 shows the effect of ASIR reconstruction on the results of the human and model observations in the 2AFC. For human observers, the use of ASIR reconstruction during low-dose abdominopelvic imaging improved the amount of PC [Figure 4a]. The amount of PC increased for a 30% reduction in radiation dose (140 mA) (83.6% ± 2% to 92.5% ± 1.5%, P = 0.001) and an 80% reduction in radiation dose (40 mA) (57.5 ± 4.3% to 86.3% ± 3.1%, P = 0.021). As in human observers, the PC values improved for the model observer for 30% (84.5 ± 1.8% to 92.7 ± 1%, P = 0.012) and 80% reductions in radiation dose (60.02 ± 3.9% to 87.33 ± 2.8%, P = 0.001) [Figure 4b]. In addition, as shown in Figure 4c and d, using the ASIR technique for reconstruction in low-dose abdominopelvic and in lung imaging increased the PC values reported by both human observers and model observers. For human observers, the amount of PC increased for both 30% (140 mA) (82 ± 1.6% to 86.39 ± 0.8%, P = 0.07) and 80% (40 mA) (54.2 ± 2.9% to 82.75 ± 2.3%, P = 0.008) reduction in radiation dose. As in human observers, in model observers, the amount of PC also increased for 30% (82.5 ± 2.6% to 86.19 ± 1.4%, P = 0.083) and 80% (56 ± 3.4% to 80.95 ± 2.9%, P = 0.001) reductions in radiation dose.

Optimization of the adaptive statistical iterative reconstruction technique to increase performance

Figure 5 shows the AUC values for objects with a contrast

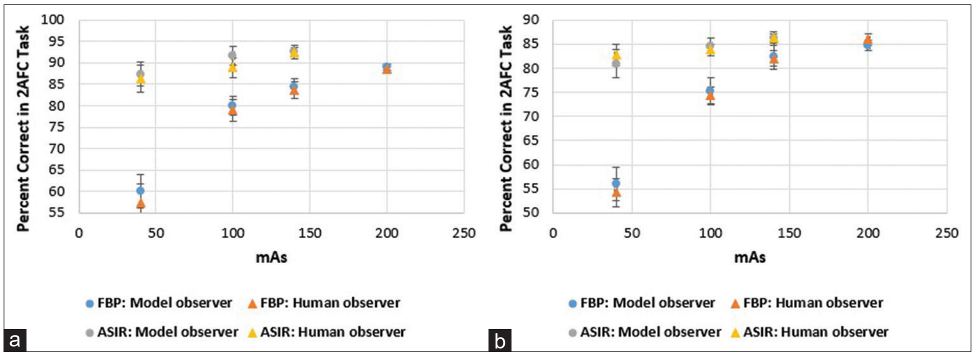

Figure 3: Percentages of correct decisions in each of the two-alternative forced choice tasks by human observers and channelized hoteling observer model observers. The two-alternative forced-choice tasks were generated at four mAs levels (40, 1 00, 140, and 200). (a) Mean area under the curve receiver operating characteristic curve in abdominopelvic images. (b) Mean area under the curve in lung images

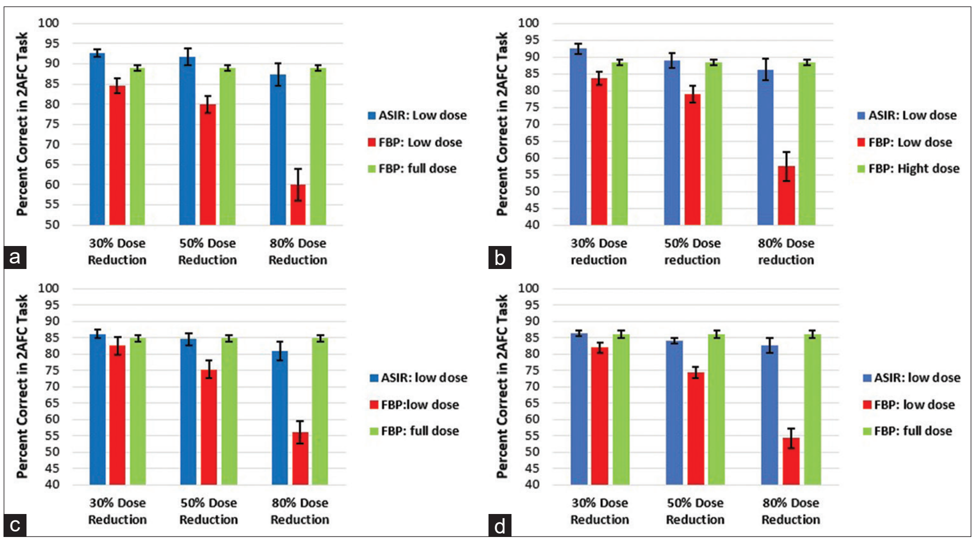

Figure 4: Area under the curve receiver operating characteristic values for high-dose filtered back projection, low-dose filtered back projection, and low-dose adaptive statistical iterative reconstruction. High-dose filtered back projection and low-dose adaptive statistical iterative reconstruction show similar area under the curve values, while low-dose filtered back-projection has a significantly lower area under the curve value. (a) Area under the curve values reported by human observers in abdominopelvic imaging. (b) Area under the curve values reported by model observers in abdominopelvic imaging. (c) Area under the curve values reported by human observers in lung imaging. (d) Area under the curve values reported by model observers in lung imaging

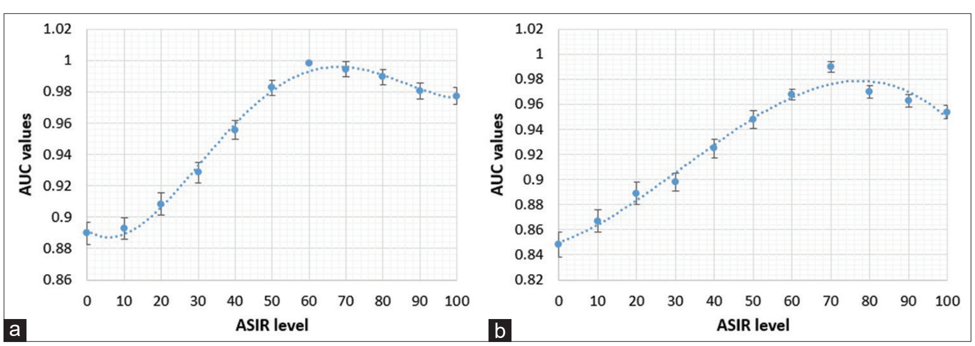

Figure 5: Area under the curve receiver operating characteristic values obtained by the channelized hoteling observer model observer for each level of adaptive statistical iterative reconstruction. (a) Mean area under the curve in abdominopelvic images. (b) Mean area under the curve in lung images

of 5 HU and a diameter of 5 mm in the FBP reconstruction method and different levels of ASIR reconstruction (from 10% to 100%) for lung and abdominopelvic imaging. Based on Figure 5a in abdominopelvic imaging, increasing the ASIR reconstruction level from 0% to 60% showed the maximum AUC (P = 0.001), while increasing the ASIR level from 0% to 70% maximized the AUC in lung imaging [Figure 5b] (P = 0.003).

Image quality assessments

The results of the image quality assessment of the abdominopelvic images by human observers are summarized in Table 3. The observers did not note any artifacts due to increased ASIR. Figure 6 shows the effect of ASIR reconstruction on the amount of noise in the abdominopelvic region of a 40-year-old patient. The amount of subjective image noise at different levels of ASIR reconstruction was equal to or less than the average noise ($P > 0.05$). Using ASIR reconstruction levels above 80% resulted in reduced image sharpness. The reliability of the diagnosis remained constant with increasing ASIR reconstruction level from 0% to 70%. The use of 90% and 100% ASIR for image reconstruction resulted in decreased detection confidence ($P < 0.05$).

In addition, the results reported by the observers showed that increasing the level of ASIR reconstruction did not significantly affect the quality of lung images. Figure 7 shows the effects of different levels of ASIR reconstruction on the amount of noise in the lung images. With an increase in the ASIR reconstruction level from 0% to 80%, the subjective image noise score was constant and equal to the average amount of noise (score 3). Using 90% and 100% ASIR improved the image noise. The sharpness and reliability of the diagnosis remained constant with increasing ASIR reconstruction level (score 3) ($P > 0.05$). No artifacts were observed in the ASIR-reconstructed lung imaging series.

Discussion

Patient radiation protection is a major issue and there is a tendency to significantly reduce the dose without sufficiently considering the potential loss of image quality. This human and model observer (CHO model) study compared the performance of different levels of ASIR and FBP in CT image quality assessment in a 2AFC task to achieve the appropriate diagnostic ability according to the patient's dose. Our results indicated that the trends of image quality provided by the CHO model were compatible with human observers.

The radiation dose can be reduced by 65%–70% in lung[21] and 31%–41% in abdominopelvic imaging, while maintaining image quality indices such as noise and spatial resolution at the standard levels.[22-24] However, our results demonstrated that

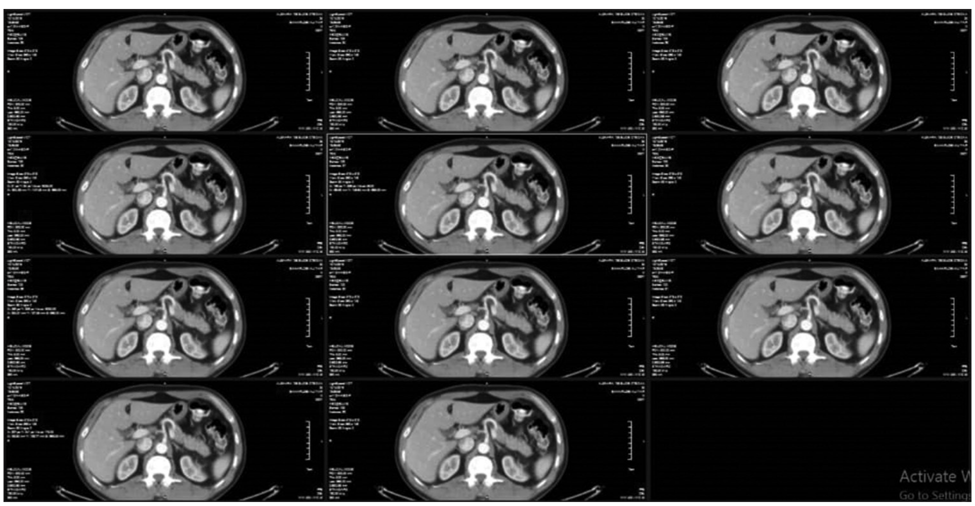

Figure 6: Transverse abdominal computed tomography images of a 40-year-old patient. Images were reconstructed with filtered back projection or adaptive statistical iterative reconstruction from 0% to 100%

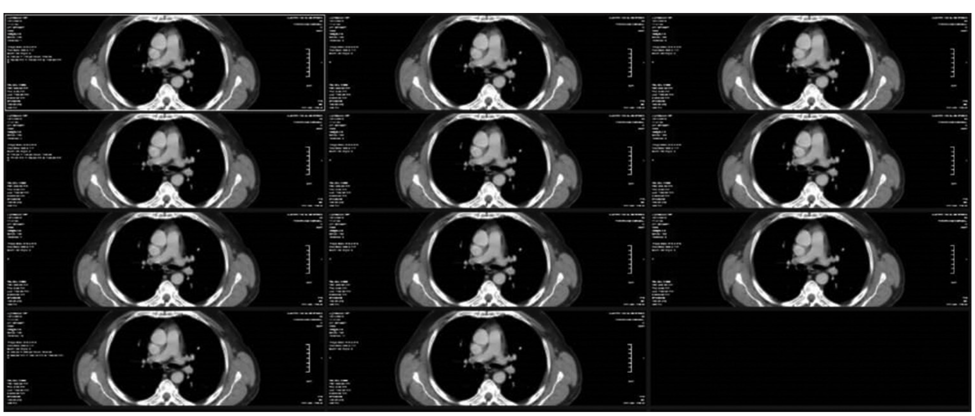

Figure 7: Transverse chest computed tomography images (lung view) of a 40-year-old patient. Images were reconstructed with filtered back projection or adaptive statistical iterative reconstruction from 0% to 100%

Table 3: Image quality assessment for abdomen-pelvic CT images reconstructed with FBP or ASIR techniques

Image reconstruction	Sharpness					Subjective image noise					Diagnostic acceptability				
	Sco1	Sco2	Sco3	Sco4	Sco5	Sco1	Sco2	Sco3	Sco4	Sco5	Sco1	Sco2	Sco3	Sco4	Sco5
FBP	-	-	100%	-	-	-	-	100%	-	-	-	-	100%	-	-
ASIR 10%	-	-	98%	-	2%	-	-	100%	-	-	-	-	94%	-	6%
ASIR 20%	-	-	98%	-	2%	-	-	100%	-	-	-	-	94%	-	6%
ASIR 30%	-	-	98%	-	2%	-	-	100%	-	-	-	-	94%	-	6%
ASIR 40%	-	-	98%	-	2%	-	-	100%	-	-	-	-	94%	-	6%
ASIR 50%	-	4%	94%	-	2%	-	-	96%	4%	-	-	-	94%	-	6%
ASIR 60%	-	8%	90%	-	2%	-	-	80%	20%	-	-	-	94%	-	6%
ASIR 70%	-	38%	60%	-	2%	-	-	50%	50%	-	-	8%	86%	2%	4%
ASIR 80%	-	68%	30%	-	2%	-	-	16%	84%	-	-	36%	58%	6%	-
ASIR 90%	-	84%	14%	2%	-	-	-	4%	96%	-	-	78%	16%	6%	-
ASIR 100%	-	92%	6%	2%	-	-	-	-	96%	4%	-	88%	6%	6%	-

although the maximum reduction of image noise was achieved with 100% ASIR, 60% ASIR in lung and abdominopelvic examinations produced optimal image quality. In other words, the use of more than 60% ASIR leads to smoother borders and reduced visibility of small, low-contrast structures. In the lung, due to the large contrast between air density and lung lesions, the level of ASIR reconstruction can be increased to improve the diagnostic value of the image. The clinical results showed that 80% and higher ASIR in the reconstruction of abdominopelvic images led to a significant reduction in sharpness and confidence in the diagnosis. In contrast, the results of clinical studies revealed that increasing the level of ASIR reconstruction led to a reduction in image noise and a gradual reduction in sharpness and diagnosis confidence.[17,18] In lung images, due to the favorable natural contrast, increasing ASIR reconstruction from 10% to 100% did not significantly affect the sharpness and diagnosis confidence.

Analysis of the NPS results showed that as the percentage of ASIR increased, the amount of noise in the spatial frequency spectrum decreased. In addition, as shown in Figure 1, the amount of noise reduction due to the increased percentage of ASIR reconstruction in the spatial frequency spectrum was not evenly distributed. The ASIR technique reduces further noise at higher spatial frequencies and results in lower noise at lower spatial frequencies. In general, the noise distribution in the spatial frequency spectrum or the appearance of noise along with the absolute magnitude of the noise can affect the image quality and, ultimately, the ability to detect low-contrast objects.[19,20] However, in terms of image quality, caution is required, particularly with the IR of the first generation tested (ASIR 50%) despite having chosen a percentage recommended to provide image quality improvement without major image texture changes.

Quantitative criteria, such as the modulation transfer function, section sensitivity profile, and NPS alone cannot be used in studies as they cannot completely describe the image quality.[25,26] In addition, some of these physical metrics are not applicable to imaging protocols. The model observer is an image quality assessment method that has been widely used in recent studies.[27] The model observer represents the conditions of an ideal observer and predicts its performance.[28] The CHO model has been applied in a variety of imaging modalities, including CT, MRI, mammography, and nuclear medicine. However, relatively few studies have examined the quality of CT images using the CHO model. Wunderlich and Noo used CHO to model human observer performance in the diagnosis of simulated lesions.[29] Solomon J *et al*. investigated the relationship between model observers and the performance of human observers for diagnostic tasks in multislice CT.[30] These studies assumed that the noise was constant and Gaussian and used computer simulations in the diagnostic task. In addition, Yu *et al*. investigated how the observer model CHO could predict human observer performance for a simple diagnostic task.[28] The present study used the CHO model to evaluate image quality. Unlike previous studies using simulated signals,[29,30] this study used low-contrast phantom scans to produce signal-absent and signal-present images. The results of this study demonstrated the excellent agreement in performance between human observers and the CHO model at different dose levels for both FBP and ASIR reconstruction methods, showing the potential of this technique to optimize radiation doses and scan protocols in clinical settings. However, placing the signals on a uniform background may simplify the decision to determine the presence of the signal in the image and the results in clinical terms may be unrealistic.

This study has some limitations. First, we did not study the impact of the scrolling speed, slice thickness, and interval. The observers were allowed to scroll back and forth at their own pace, consistent with the realistic reading of patient images. Slice thickness and interval may also affect observer performance during multislice scrolling, which requires additional research. Second, 2AFC is the simplest form of localization (observers choose from two possible locations).

Conclusions

The results of this study showed that a 60% ASIR in images of the lungs, abdomen, and pelvis improved the image quality.

Additionally, 80% ASIR for imaging of these regions reduced the radiation dose by 80% while maintaining the image quality.

Acknowledgments

This study was supported by Isfahan University of Medical Sciences, Grant #297172. We thank our colleagues from Alzahra Hospital management who provided insight and expertise that greatly assisted the research.

Financial support and sponsorship

Nil.

Conflicts of interest

There are no conflicts of interest.

References

1. Elmokadem AH, Ibrahim EA, Gouda WA, Khalek Abdel Razek AA. Whole-body computed tomography using low-dose biphasic injection protocol with adaptive statistical iterative reconstruction V: Assessment of dose reduction and image quality in trauma patients. J Comput Assist Tomogr 2019;43:870-6.
2. Lee NK, Kim S, Hong SB, Kim TU, Ryu H, Lee JW, *et al.* Low-dose CT with the adaptive statistical iterative reconstruction V technique in abdominal organ injury: Comparison with routine-dose CT with filtered back projection. AJR Am J Roentgenol 2019;213:659-66.
3. Widmann G, Juranek D, Waldenberger F, Schullian P, Dennhardt A, Hoermann R, *et al.* Influence of ultra-low-dose and iterative reconstructions on the visualization of orbital soft tissues on maxillofacial CT. AJNR Am J Neuroradiol 2017;38:1630-5.
4. Power SP, Moloney F, Twomey M, James K, O'Connor OJ, Maher MM. Computed tomography and patient risk: Facts, perceptions and uncertainties. World J Radiol 2016;8:902-15.
5. Patro SN, Chakraborty S, Sheikh A. The use of adaptive statistical iterative reconstruction (ASiR) technique in evaluation of patients with cervical spine trauma: Impact on radiation dose reduction and image quality. Br J Radiol 2016;89:20150082.
6. Jensen CT, Liu X, Tamm EP, Chandler AG, Sun J, Morani AC, *et al.* Image quality assessment of abdominal CT by use of new deep learning image reconstruction: Initial experience. AJR Am J Roentgenol 2020;215:50-7.
7. Han WK, Na JC, Park SY. Low-dose CT angiography using ASiR-V for potential living renal donors: A prospective analysis of image quality and diagnostic accuracy. Eur Radiol 2020;30:798-805.
8. Kahn J, Kaul D, Böning G, Rotzinger R, Freyhardt P, Schwabe P, *et al*. Quality and dose optimized CT trauma protocol–recommendation from a university level-I trauma center. In: RöFo-Fortschritte auf dem Gebiet der Röntgenstrahlen und der bildgebenden Verfahren. Vol. 189. © Georg Thieme Verlag KG; 2017. p. 844-54.
9. Alagic Z, Eriksson A, Drageryd E, Motamed SR, Wick MC. A new low-dose multi-phase trauma CT protocol and its impact on diagnostic assessment and radiation dose in multi-trauma patients. Emerg Radiol 2017;24:509-18.
10. Chen LH, Jin C, Li JY, Wang GL, Jia YJ, Duan HF, *et al.* Image quality comparison of two adaptive statistical iterative reconstruction (ASiR, ASiR-V) algorithms and filtered back projection in routine liver CT. Br J Radiol 2018;91:20170655.
11. Rotzinger DC, Racine D, Beigelman-Aubry C, Alfudhili KM, Keller N, Monnin P, *et al.* Task-based model observer assessment of a partial model-based iterative reconstruction algorithm in thoracic oncologic multidetector CT. Sci Rep 2018;8:17734.
12. Euler A, Solomon J, Marin D, Nelson RC, Samei E. A third-generation adaptive statistical iterative reconstruction technique: Phantom study of image noise, spatial resolution, lesion detectability, and dose reduction potential. AJR Am J Roentgenol 2018;210:1301-8.
13. Ge D, Zhang L, Cavaro-Ménard C, Le Callet P. Numerical stability issues on channelized hotelling observer under different background assumptions. J Opt Soc Am A Opt Image Sci Vis 2014;31:1112-7.
14. Zhou W, Li H, Anastasio MA. Approximating the ideal observer and hotelling observer for binary signal detection tasks by use of supervised learning methods. IEEE Trans Med Imaging 2019;38:2456-68.
15. Kim G, Han M, Shim H, Baek J. A convolutional neural network-based model observer for breast CT images. Med Phys 2020;47:1619-32.
16. Singh S, Kalra MK, Gilman MD, Hsieh J, Pien HH, Digumarthy SR, *et al.* Adaptive statistical iterative reconstruction technique for radiation dose reduction in chest CT: A pilot study. Radiology 2011;259:565-73.
17. Sagara Y, Hara AK, Pavlicek W, Silva AC, Paden RG, Wu Q. Abdominal CT: Comparison of low-dose CT with adaptive statistical iterative reconstruction and routine-dose CT with filtered back projection in 53 patients. AJR Am J Roentgenol 2010;195:713-9.
18. Shah SM, Deep K, Siramanakul C, Mahajan V, Picard F, Allen DJ. Computer navigation helps reduce the incidence of noise after ceramic-on-ceramic total hip arthroplasty. J Arthroplasty 2017;32:2783-7.
19. Lee E, Kim DS. Precision analysis of the noise power spectrum estimate in radiography imaging. In: Medical Imaging 2018: Physics of Medical Imaging. Vol. 10573. SPIE; 2018. p. 1550-7.
20. Metheany KG, Abbey CK, Packard N, Boone JM. Characterizing anatomical variability in breast CT images. Med Phys 2008;35:4685-94.
21. Lee SH, Kim MJ, Yoon CS, Lee MJ. Radiation dose reduction with the adaptive statistical iterative reconstruction (ASIR) technique for chest CT in children: An intra-individual comparison. Eur J Radiol 2012;81:e938-43.
22. Deák Z, Grimm JM, Treitl M, Geyer LL, Linsenmaier U, Körner M, *et al.* Filtered back projection, adaptive statistical iterative reconstruction, and a model-based iterative reconstruction in abdominal CT: An experimental clinical study. Radiology 2013;266:197-206.
23. Prezzi D, Owczarczyk K, Bassett P, Siddique M, Breen DJ, Cook GJ, *et al.* Adaptive statistical iterative reconstruction (ASIR) affects CT radiomics quantification in primary colorectal cancer. Eur Radiol 2019;29:5227-35.
24. Gatti M, Marchisio F, Fronda M, Rampado O, Faletti R, Bergamasco L, *et al.* Adaptive statistical iterative reconstruction-V versus adaptive statistical iterative reconstruction: Impact on dose reduction and image quality in body computed tomography. J Comput Assist Tomogr 2018;42:191-6.
25. Kazerooni EA, Armstrong MR, Amorosa JK, Hernandez D, Liebscher LA, Nath H, *et al.* ACR CT accreditation program and the lung cancer screening program designation. J Am Coll Radiol 2015;12:38-42.
26. Siewerdsen J, Cunningham I, Jaffray D. A framework for noise-power spectrum analysis of multidimensional images. Med Phys 2002;29:2655-71.
27. Bellesi L, Wyttenbach R, Gaudino D, Colleoni P, Pupillo F, Carrara M, *et al.* A simple method for low-contrast detectability, image quality and dose optimisation with CT iterative reconstruction algorithms and model observers. Eur Radiol Exp 2017;1:18.
28. Yu L, Leng S, Chen L, Kofler JM, Carter RE, McCollough CH. Prediction of human observer performance in a 2-alternative forced choice low-contrast detection task using channelized hotelling observer: Impact of radiation dose and reconstruction algorithms. Med Phys 2013;40:041908.
29. Solomon J, Samei E. Correlation between human detection accuracy and observer model-based image quality metrics in computed tomography. J Med Imaging (Bellingham) 2016;3:035506.
30. Noferini L, Taddeucci A, Bartolini M, Bruschi A, Menchi I. CT image quality assessment by a Channelized Hotelling Observer (CHO): Application to protocol optimization. Phys Med 2016;32:1717-23.